



Research article

Fault detection of rolling bearing based on principal component analysis and empirical mode decomposition

Yu Yuan^{1,3,*} and Chen Chen²

¹ School of Locomotive and Rolling Stock Engineering, Dalian Jiaotong University, Dalian 116028, China

² School of Mechanical Engineering, Dalian Jiaotong University, Dalian 116028, China

³ Traction Power State Key Laboratory of Southwest Jiaotong University, Chendu 610031, China

* **Correspondence:** Email: Yuanyu_knife@163.com.

Abstract: For the problem of inconsistent quantitative standards for running status analysis of rolling bearings, this paper uses principal component analysis (PCA) to extract a new index F, which is the joint parameters of time domain and frequency domain, and by establishing the value of F to analyze the running states of the rolling bearings. Firstly, the acceleration sensors are used to collect the vibration signal of the whole life cycle of the rolling bearings. Secondly, empirical mode decomposition (EMD) method is used to denoise the acquired vibration signal. Then, the main components of the denoised vibration signal are used to propose the characteristic parameters and synthesized into new parameter indicators. Finally, envelope analysis spectrum is used to analyze the fault classification under the new parameter index. The experiment results show that the whole life cycle of the rolling bearings can be classified into five different operating periods by using the new parameter index, and each period represents a different bearing operating state.

Keywords: rolling bearing; PAC; life cycle; EMD; envelope analysis

Mathematics Subject Classification: 03C98, 62H25

1. Introduction

The rolling bearings are key components of rotary machines, they also create a variety of faults. These failures can lead to downtime and huge economic losses [1–3]. According to the current

statistical data, it can be known that about one-third of the malfunctions of rotary machines are caused by bearing failures [4–7]. Therefore, it is necessary to monitor bearing condition efficiently [8–10].

Bearing failure is a multi-state process. The state in this process cannot be observed directly. Therefore, the measurement signals require professional analysis [11–14]. The majority of common intelligent fault diagnosis systems are built on the basis of feature extraction of monitoring signals [15]. Traditional feature signal extraction method mainly include wavelet transform (WT) [12,13], Hilbert Huang Transform (HHT) [16], empirical mode decomposition (EMD) [17], variational mode decompositions (VMD) [18]. Lu et al. [19] introduced a novel feature extraction method using adaptive multi-wavelets based on genetic algorithm and the synthetic detection index. Zheng et al. [20] analyzed an adaptive parameterless empirical wavelet transform and normalized Hilbert transform for rotor rubbing fault diagnosis. Cheng et al. [21] presented a new fault diagnosis method based on deep learning and Hilbert transform for the drivetrain gearboxes. For the study of bearing life, Ocak et al. [22] proposed HMM-based fault detection and diagnosis of rolling bearings. Gebraeel [23] studied residual life predictions from vibration-based degradation signals. Sun et al. [24] applied SVM technology in life prediction to improve prediction accuracy. Vlok et al. [25] analyzed the use of statistical residual life estimates of bearings to quantify the influence of preventive maintenance actions. A Hidden Markov Models is introduced into the prediction of bearing fatigue life in [26,27], and achieved a good analysis effect. Shao et al. [28] studied using the kurtosis index and the root mean square value as the characteristic parameters of the collected vibration signals, and used the neural network to predict the bearing vibration characteristics, but the progress in life prediction was not smooth. Ben et al. [29] combined the neural network and Weibull distribution to predict the bearing life, which defined six degradation states of the bearing. The other optimization algorithms are used to combine with signal processing methods [30–41].

Based on the above analysis, it has been found that there are three main problems in the research of bearing life: the acquisition of bearing operation life cycle data, the choice of parameters for the study of bearing operation status, and the selection of prediction models. Aiming at these problems, this paper proposes corresponding solutions. Firstly, the experimental data is acquired through an experimental device. Then, a new parameter index F for bearing life analysis is proposed. Finally, the new parameter index F is used to divide the bearing life states.

2. Signal selection

To accurately predict bearing life, data selection is crucial. The monitoring of the bearing's operating conditions can usually be oil sample analysis, temperature monitoring, vibration monitoring [42]. The oil sample analysis method is only applicable to bearings with oil lubrication, and is not suitable for bearings with grease lubrication. At the same time, this method is easily affected by other non-bearing component, so it has greater limitations. Temperature monitoring will only increase the temperature obviously when the bearing failure reaches a certain level, but in the early stage of the bearings failure, the bearings temperature is almost unaffected; Vibration monitoring uses sensors to collect signals, and then analyzes the current running status of the bearings based on the collected signals. Under different working conditions, the bearing's vibration

data graphic form is different, which has a good discrimination effect. Therefore, this paper adopts vibration monitoring and selects the bearing vibration data as the analysis basis. The vibration signals collected by rolling bearings under different operating conditions are shown in Figure 1.

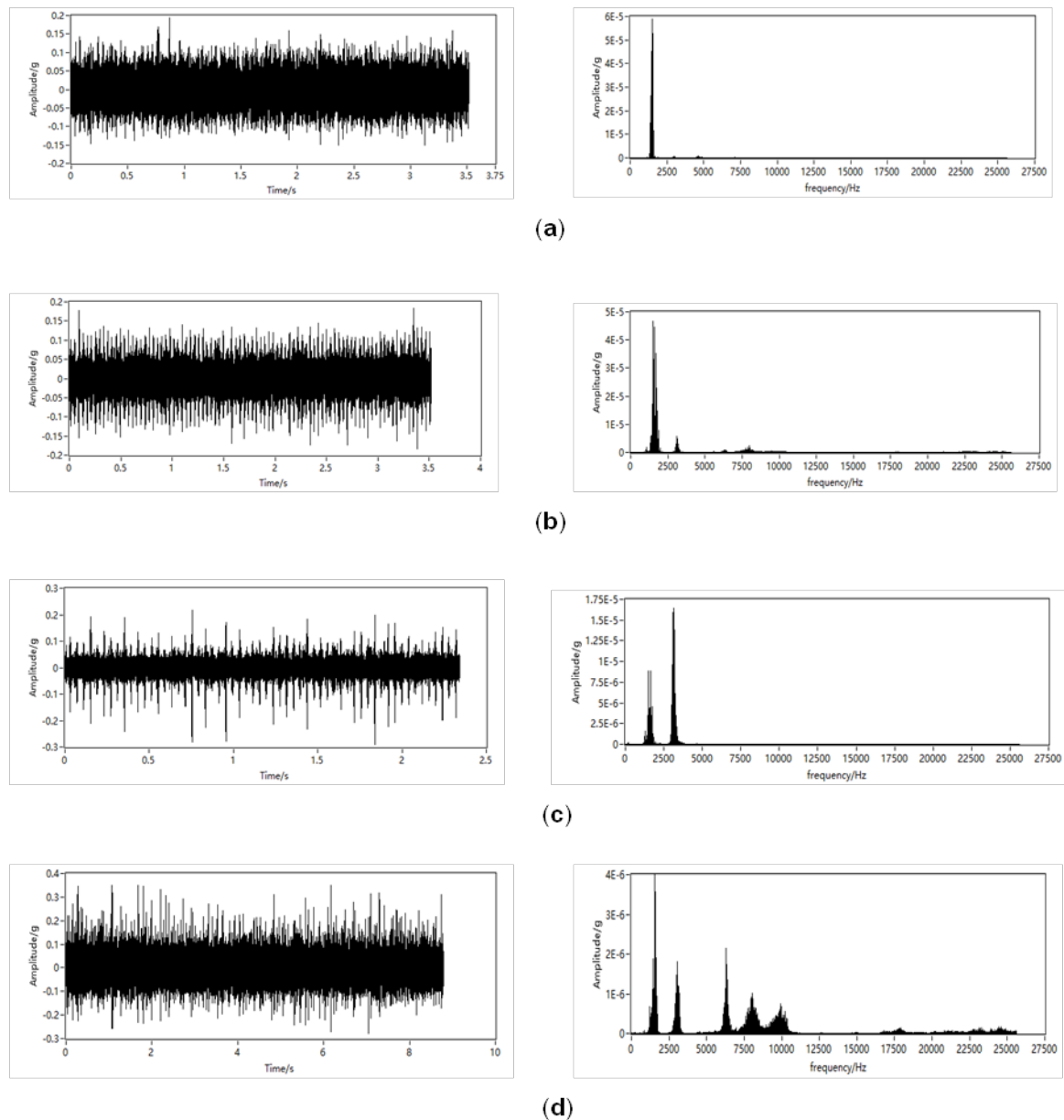


Figure 1. Vibration data of rolling bearings at different times. (a) Normal state vibration signal, (b) Early fault vibration signal, (c) Medium-term fault vibration signal, (d) vibration signal in the end of life.

It can be concluded from Figure 1 that under different working conditions, there is a significant difference in the vibration data of rolling bearings, which is beneficial for determining the operating status of the bearings. So it is reliable to use the vibration signal data as the analysis data.

In the study of this paper, the time interval of collected vibration data is ten minutes, each sampling data is 180,000, among them the rolling bearing used is N205, the rotational speed is 1500 rad/min.

3. Signal denoising

In the EMD, we can decompose an original signal into several Intrinsic Mode Function (IMF) components. By using the correlation coefficient between the IMF component and the original signal, we can discriminate useful and pseudo-components. At the same time, we can also distinguish some noise components through the correlation coefficient. Studies have shown that white noise is irrelevant to any signal, so it can be known that the correlation between the IMF component produced by the noise and the original signal is small, which allows us to easily eliminate the noise components and retain useful actual signal components.

We can obey the following two principles can be obeyed to determine whether it is a noise signal in the EMD:

- (i) Cross-correlation analysis. The cross-correlation between the white noise and the original signal is zero. When judging the noise signal, if the derived component has a small correlation coefficient with the original signal, this component may be a noise component.
- (ii) Autocorrelation analysis. White noise autocorrelation usually achieves a maximum on the axis of symmetry and the rest are zero. Therefore, it may be that the component of the noise signal obtained in (1) is further subjected to autocorrelation calculation. If the maximum value is obtained on the axis of symmetry and other values are small, the component may be determined as noise.

Judging from the above two principles, we can eliminate the noise signal in the EMD decomposition to achieve signal denoising (Figure 2).

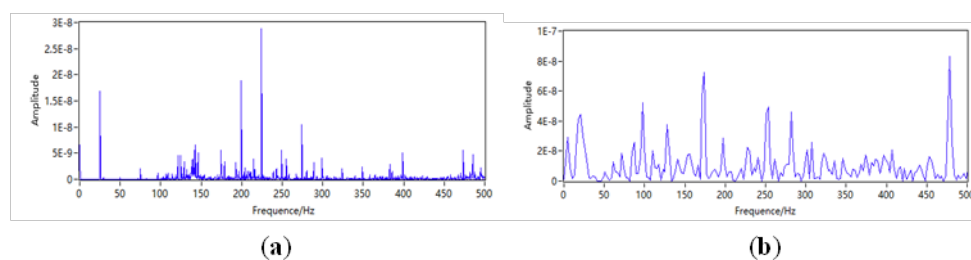


Figure 2. Comparison between EMD denoised signal and original signal. (a) Raw signal power spectrum, (b) EMD denoising signal power spectrum.

4. Analysis of characteristic parameters of rolling bearings

4.1. Analysis of time domain characteristic parameters of rolling bearings

If an abnormal situation occurs in the rolling bearing during operation, some statistics of the time domain parameters of the vibration signal can reflect the characteristic information of the fault signal to a certain extent. We select the maximum value, minimum value, peak-to-peak value, mean

value, variance, standard deviation, root mean square (RMS) value, skewness, crest factor, kurtosis value, and degree of skewness in the time domain parameters as the basis for judging whether the bearing has failed [43].

By analyzing the experimental data, the overall trend of the entire life cycle of traditional time domain indicators are shown in Figure 3.

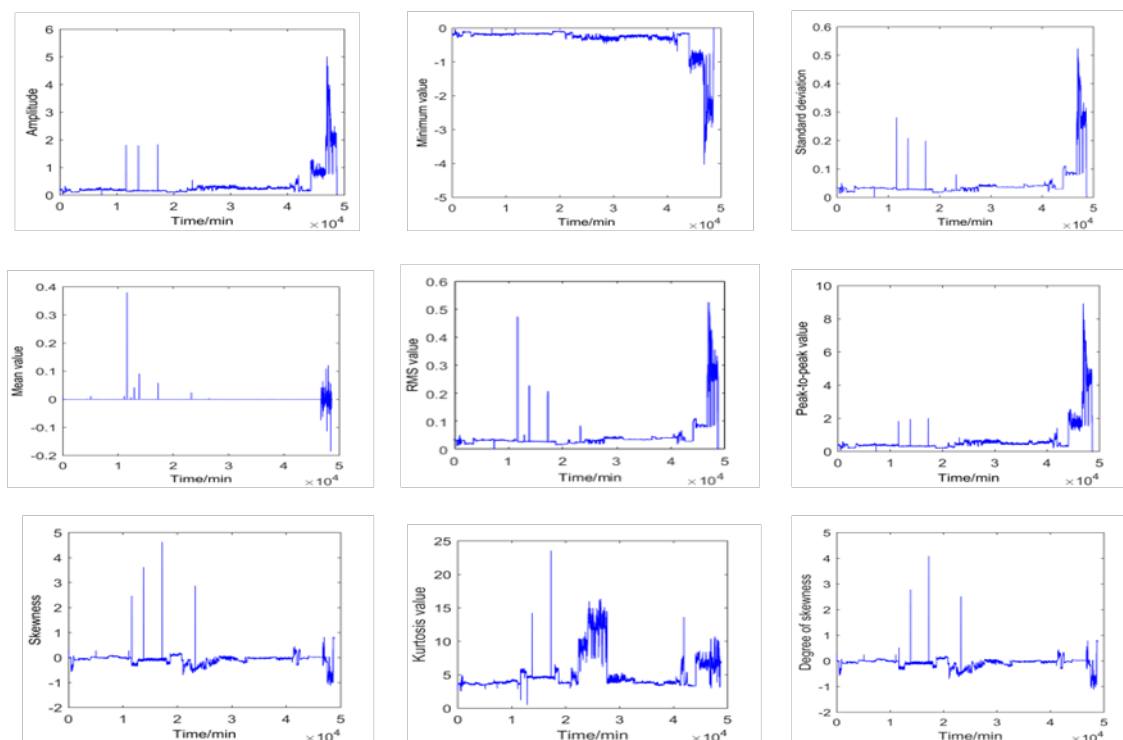


Figure 3. Trend of time domain parameter indicators.

As can be seen from Figure 3, the maximum value, minimum value, standard deviation, RMS value, and peak-to-peak values of the traditional time domain parameter indicators perform better at the end of the full life of the rolling bearing. Skewness indicator fluctuates significantly in the middle of the full life of the rolling bearing, and there are some differences at the end. The kurtosis value indicator performs the best in all indicators, and the parameter amplitude has changed significantly throughout the middle and end of the whole life. In summary, different time domain parameter indexes have their own advantages and disadvantages, but as far as the whole life cycle is concerned, no time domain parameter index can fully represent the changing trend of the entire life of the rolling bearings.

4.2. Analysis of frequency domain characteristic parameters of rolling bearings

Using the characteristic parameters in the frequency domain to describe the running status of rolling bearings is also a universal monitoring method. Its characteristic parameters are usually statistical functions, such as frequency domain average, center of gravity frequency, mean square frequency, frequency domain amplitude variance, frequency domain amplitude standard deviation,

frequency domain amplitude deviation index, frequency domain amplitude kurtosis index. The time domain signal is converted into the frequency domain range by Fourier change, then the bearings fault and variation trend can be judged by the change of the frequency component.

Based on experimental data, the overall trend of the traditional frequency domain indicators over the entire life cycle are shown in Figure 4.

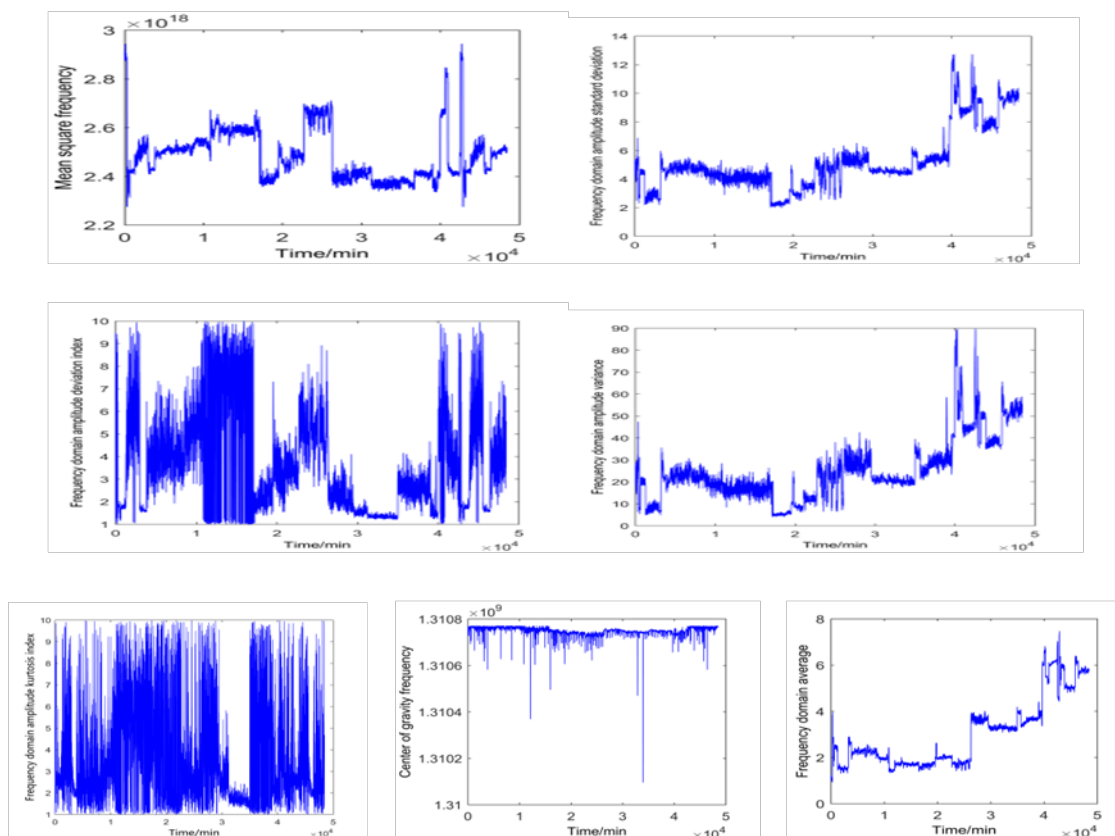


Figure 4. Trend of frequency domain parameter indicators.

It can be known from Figure 4 that under the frequency domain index of the rolling bearings full life cycle data, the frequency domain amplitude deviation index and the frequency domain amplitude kurtosis index have large fluctuations. Center of gravity frequency is stable throughout the life cycle. The mean square frequency is significantly different in the early and middle stages of life. Throughout the entire life cycle, the frequency domain amplitude standard deviation, frequency domain amplitude variance, and frequency domain average have obvious state changes. To sum up, although some parameters have a good distinction between the running status of the bearings, but in terms of the entire life states, no one indicator can fully represent the entire change trend of the rolling bearings.

In summary, the traditional time domain indicators perform well at the end of their full life, while the frequency domain indicators have certain advantages in the middle. Therefore, a new judgment indicator needs to be proposed, which can complement the advantages of the two.

5. Feature parameter extraction based on PCA

Principal component analysis (PCA) is mainly a linear multivariate statistical analysis method that selects a few variables from multiple variables, and the selected few variables can still represent most of the original variables. The original multiple variables are likely to be relevant, but the selected few variables after the PCA are irrelevant. From the perspective of mathematics, the selection of variables in PCA is actually the idea of dimension reduction. That is to reduce the number of variables in bearing fault diagnosis, and select the representative parameter variables that can analyze bearing failure [44,45].

5.1. Analysis steps

In the PCA, an $n \times m$ matrix needs to be established and named X, n indicates the number of data, m represents the number of original variables [46,47].

$$X = \begin{bmatrix} x_{11} & x_{12} & \dots & x_{1m} \\ x_{21} & x_{22} & \dots & x_{2m} \\ \dots & \dots & \dots & \dots \\ x_{n1} & x_{n2} & \dots & x_{nm} \end{bmatrix} = [X_1, X_2, \dots, X_m] \quad (1)$$

In order to eliminate the impact of dimension on modeling, the formula for data normalization is:

$$X_{i \times j} = \frac{x_{i \times j} - x_{j-\min}}{x_{j-\max} - x_{j-\min}} \quad (2)$$

The singular value (eigenvalue) decomposition of the above covariance matrix is as follows:

$$COV(X) = P \begin{bmatrix} \lambda_1 & 0 \\ 0 & \lambda_m \end{bmatrix} P^T = \sum_{i=1}^m \lambda_i P_i P_i^T \quad (3)$$

$$COV(X)P_i = \lambda_i P_i$$

where $\lambda_1, \lambda_2, \dots, \lambda_m$ are the eigenvalues of the covariance matrix arranged in descending order, that is, $\lambda_1 \geq \lambda_2 \geq \dots \geq \lambda_m$. P_1, P_2, \dots, P_m are feature vectors corresponding to each feature value. The normalized matrix is decomposed with eigenvectors as shown in Eq (4).

$$\hat{X} = t_1 P_1^T + t_2 P_2^T + \dots + t_k P_k^T + E = TP^T + E \quad (4)$$

where T is the score matrix, P represents the load matrix, t_i is the score vector, k is the number of principal elements, E is the residual matrix, which indicates redundant information and noise in the

original data. In the PCA, the score vector is orthogonal to each other. The load vector is also orthogonal to each other, and the length of each load vector is 1. Eq (5) will be obtained by multiplying both sides of Eq (4) by P_i .

$$XP_i = t_1 P_1^T P_i + t_2 P_2^T P_i + \mathbf{L} + t_m P_m^T P_i \quad (5)$$

So $t_i = XP_i$. The above formula shows that the score vector is essentially the projection of the data matrix X on its corresponding load vector square. According to the length, the score vector can be arranged as follows:

$$\|t_1\| > \|t_2\| > \mathbf{L} > \|t_m\| \quad (6)$$

Because the error matrix E is mainly caused by measurement errors, ignoring E can have the effect of removing noise and will not cause the loss of useful information in the data. In a word, the essence of the PCA of data is to consider the process of the projection of the data matrix on its load vector, that is, to reduce the m -dimensional data variable to the k -dimensional data variable by using the projection transformation. Therefore, the data X can be approximated by the following formula:

$$X' = t_1 P_1^T + t_2 P_2^T + \mathbf{L} + t_k P_k^T \quad (7)$$

The basis for selecting the number of principal components is to calculate the cumulative degree of the number of principal components to the data. If the cumulative contribution rate of the first k principal components exceeds a threshold value of 0.85, it can be considered that it is feasible to extract the first k principal components as comprehensive indicators. Therefore, the original m -dimensional space becomes a k -dimensional space, which plays a role in dimension reduction.

$$\sum_{i=1}^k \lambda_i \div \sum_{i=1}^m \lambda_i \geq 85\% \quad (8)$$

The comprehensive indicator F_k is extracted, which can reflect the information possessed by the original multiple variables to the greatest extent, and at the same time, it must be ensured that the information of a few new indicators does not overlap and is not relevant.

$$F_1 = a_{11}X_1 + a_{21}X_2 + \mathbf{L} + a_{m1}X_m \quad (8)$$

where F_1 refers to the principal component index composed of the first linear combination in the original data, which contains the largest amount of information. The largest linear combination of X_1, X_2, \dots, X_m among many linear combinations of X_1, X_2, \dots, X_m is selected as F_1 , and F_1 is called the first principal component. If the first principal component cannot fully represent the characteristic information of the original m indicators, the second principal component F_2 needs to be considered,

Table 2. Component matrix.

Parameter index	Ingredients			
	1	2	3	4
Maximum value	0.975	-0.060	0.047	-0.177
Minimum value	-0.843	0.429	-0.013	0.297
Peak-to-peak value	0.939	-0.240	0.032	-0.240
Mean value	0.464	0.605	-0.241	0.558
Variance	0.789	0.324	-0.306	0.350
Standard deviation	0.984	0.042	-0.132	-0.062
RMS value	0.977	0.108	-0.163	0.013
Skewness	0.113	0.878	0.391	-0.239
Crest factor	0.377	-0.305	0.749	0.194
Kurtosis value	0.287	-0.253	0.710	0.461
Degree of skewness	0.059	0.854	0.408	-0.304

The main formulas and fusion parameter formulas can be obtained from Table 1 and Table 2:

$$\begin{aligned}
 F_1 &= 0.975x_1 - 0.843x_2 + 0.939x_3 + 0.464x_4 + 0.789x_5 + 0.984x_6 \\
 &\quad + 0.977x_7 + 0.113x_8 + 0.377x_9 + 0.287x_{10} + 0.059x_{11} \\
 F_2 &= -0.06x_1 + 0.429x_2 - 0.24x_3 + 0.605x_4 + 0.324x_5 + 0.042x_6 \\
 &\quad + 0.108x_7 + 0.878x_8 - 0.305x_9 - 0.253x_{10} + 0.854x_{11} \\
 F_3 &= 0.047x_1 - 0.013x_2 + 0.032x_3 - 0.241x_4 - 0.306x_5 - 0.132x_6 \\
 &\quad - 0.163x_7 + 0.931x_8 + 0.749x_9 + 0.710x_{10} + 0.408x_{11} \\
 F_4 &= -0.177x_1 + 0.297x_2 - 0.240x_3 + 0.558x_4 + 0.350x_5 - 0.062x_6 \\
 &\quad + 0.013x_7 - 0.239x_8 + 0.194x_9 + 0.461x_{10} - 0.304x_{11} \\
 F &= \frac{50.417\% F_1 + 21.694\% F_2 + 12.392\% F_3 + 11.224\% F_4}{95.726\%}
 \end{aligned} \tag{11}$$

Since the new feature parameter F is formed by combining the original feature parameters through a linear operation, the new parameter F contains the features of the original parameters, and the performance of these parameters is combined to provide better feedback [49]. The trend chart of the new parameter index F in the whole life cycle is shown in Figure 5.

It can be seen from Figure 5 that the parameter index F extracted by PCA can divide the bearing state into four stages throughout the entire life cycle of the rolling bearings. However, as far as Figure 5 is concerned, the second and third phases should be relative to the three operating states of the bearings, namely normal operation, early failure, and intermediate failure. The parameter indicators extracted in the time domain cannot effectively divide them. Therefore it is limited to consider only time domain parameters.

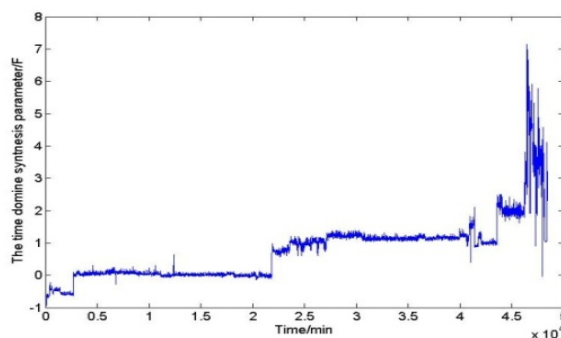


Figure 5. Trend of time domain synthesis parameter F .

5.3. Extraction of frequency domain characteristic parameter indicators

For the collected cycle life data of rolling bearing N205, the frequency domain average value, center of gravity frequency, mean square frequency, frequency domain amplitude variance, frequency domain amplitude standard deviation, frequency domain amplitude deviation index, and frequency domain amplitude are selected as frequency domain analysis variables, which is $m = 7$. By using Statistical Package for the Social Sciences (SPSS) software, the principal components of the frequency domain characteristic parameters of the rolling bearings are decomposed. The results are shown in Table 3 and Table 4.

Table 3. Total variance explained.

Ingredi-ents	Initial feature value			Extract square and load		
	Total	Variance (%)	Grand total (%)	Total	Variance (%)	Grand total (%)
1	2.779	39.701	39.701	2.779	39.701	39.701
2	1.595	22.784	62.485	1.595	22.784	62.485
3	1.339	19.124	81.608	1.339	19.124	81.608
4	0.855	12.218	93.826	0.855	12.218	93.826
5	0.338	4.830	98.656	—	—	—
6	0.083	1.181	99.836	—	—	—
7	0.011	0.164	100.000	—	—	—

Table 4. Component matrix.

Parameter index	Ingredients			
	1	2	3	4
Frequency domain average	0.659	-0.179	0.481	0.401
Center of gravity frequency	-0.664	0.171	0.683	0.165
Mean square frequency	-0.625	0.546	0.508	-0.094
Frequency domain amplitude variance	0.853	0.430	0.213	-0.076
Frequency domain amplitude standard deviation	0.866	0.426	0.197	-0.077
Frequency domain amplitude deviation index	-0.120	0.814	-0.367	-0.233
Frequency domain amplitude kurtosis index	-0.143	0.455	-0.405	0.770

The main formulas and fusion parameter formulas can be obtained from Table 3 and Table 4:

$$\begin{aligned}
 F_1 &= 0.695x_1 - 0.664x_2 - 0.625x_3 + 0.853x_4 + 0.866x_5 - 0.12x_6 - 0.143x_7 \\
 F_2 &= -0.179x_1 + 0.171x_2 + 0.546x_3 + 0.43x_4 + 0.426x_5 + 0.814x_6 + 0.455x_7 \\
 F_3 &= 0.481x_1 + 0.683x_2 + 0.508x_3 + 0.213x_4 + 0.197x_5 - 0.367x_6 - 0.405x_7 \\
 F_4 &= 0.401x_1 + 0.165x_2 - 0.094x_3 - 0.076x_4 - 0.077x_5 - 0.233x_6 + 0.77x_7 \\
 F &= \frac{39.701\%F_1 + 22.784\%F_2 + 19.124\%F_3 + 12.218\%F_4}{93.826\%}
 \end{aligned} \tag{12}$$

The trend graph of the new frequency domain parameter variable F throughout the life cycle is shown in Figure 6.

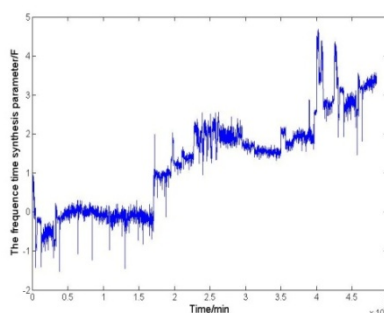


Figure 6. Trend of frequency domain synthesis parameter F .

According to Figure 6, it can be seen that the frequency domain parameter index F extracted by PCA can divide the bearing state into four stages throughout the entire life cycle of the rolling bearings, and the values of each stage have significant differences. However, in the first stage, the rolling bearing has two states: running-in period and normal operation. The parameter index extracted in the frequency domain cannot effectively divide it. Therefore, considering only the frequency domain parameters has limitations.

In order to make a better judgment of the entire life of the bearing, consider the joint analysis of time domain parameters and frequency domain parameters to make up for each other's deficiencies, which can improve the accuracy of the parameter indicators to determine the life cycle of the bearings.

5.4. Extraction of joint feature parameters in time domain and frequency domain

When performing joint characteristic parameters in the time domain and frequency domain, the principal components are extracted simultaneously from 11 parameters in the time domain and 7 parameters in the frequency domain. Then the PCA was performed by SPSS software. The results are shown in Table 5 and Table 6.

Table 5. Total variance explained.

Ingredients	Initial feature value			Extract square and load		
	Total	Variance (%)	Grand total (%)	Total	Variance (%)	Grand total (%)
1	5.665	31.474	31.474	5.665	31.474	31.474
2	2.747	15.262	46.736	2.747	15.262	46.736
3	2.355	13.086	59.822	2.355	13.086	59.822
4	1.676	9.309	69.131	1.676	9.309	69.131
5	1.494	8.302	77.433	1.494	8.302	77.433
6	1.368	7.602	85.035	1.368	7.602	85.035
7	0.958	5.322	90.357	—	—	—
8	0.824	4.580	94.936	—	—	—
9	0.363	2.016	96.953	—	—	—
10	0.266	1.478	98.430	—	—	—
11	0.146	0.811	99.241	—	—	—
12	0.076	0.425	99.665	—	—	—
13	0.024	0.134	99.800	—	—	—
14	0.015	0.086	99.885	—	—	—
15	0.013	0.075	99.960	—	—	—
16	0.006	0.032	99.993	—	—	—
17	0.001	0.007	100.000	—	—	—
18	1.009E-013	1.048E-013	100.000	—	—	—

Table 6. Component matrix.

Parameter index	Ingredients					
	1	2	3	4	5	6
Maximum value	0.980	0.032	-0.028	-0.025	0.031	-0.005
Minimum value	-0.881	0.088	0.354	0.069	-0.018	0.012
Peak-to-peak value	0.956	-0.026	-0.187	-0.047	0.025	-0.009
Mean value	0.385	0.189	0.580	-0.014	-0.209	0.039
Variance	0.809	0.105	0.249	-0.073	-0.279	0.011
Standard deviation	0.983	0.026	0.035	-0.076	-0.119	0.006
RMS value	0.978	0.042	0.087	-0.076	-0.144	0.009
Skewness	0.085	0.217	0.890	0.112	0.280	0.045
Crest factor	0.394	0.054	-0.255	0.233	0.746	0.055
Kurtosis value	0.300	0.181	-0.248	0.445	0.605	-0.037
Degree of skewness	0.038	0.201	0.870	0.102	0.298	0.044
Frequency domain average	-0.014	-0.633	0.151	-0.150	0.117	0.501
Center of gravity frequency	-0.072	0.622	-0.153	0.076	-0.165	0.701
Mean square frequency	-0.038	0.615	-0.202	0.471	-0.209	0.514
Frequency domain amplitude variance	0.124	-0.813	0.104	0.458	-0.123	0.215
Frequency domain amplitude standard deviation	0.116	-0.826	0.111	0.456	-0.120	0.197
Frequency domain amplitude deviation index	0.031	0.162	0.000	0.744	-0.301	-0.358
Frequency domain amplitude kurtosis index	-0.019	0.171	0.038	0.394	-0.206	-0.373

The main formulas and fusion parameter formulas can be obtained from Table 5 and Table 6:

$$\begin{aligned}
 F_1 &= 0.98x_1 - 0.881x_2 + 0.956x_3 + 0.385x_4 + 0.809x_5 + 0.983x_6 + 0.978x_7 \\
 &\quad + 0.085x_8 + 0.394x_9 + 0.300x_{10} + 0.038x_{11} - 0.014x_{12} - 0.072x_{13} \\
 &\quad - 0.038x_{14} + 0.124x_{15} + 0.116x_{16} + 0.031x_{17} - 0.019x_{18} \\
 F_2 &= 0.032x_1 + 0.088x_2 - 0.026x_3 + 0.189x_4 + 0.105x_5 + 0.026x_6 + 0.042x_7 \\
 &\quad + 0.217x_8 + 0.054x_9 + 0.181x_{10} + 0.201x_{11} - 0.633x_{12} + 0.622x_{13} \\
 &\quad + 0.615x_{14} - 0.813x_{15} - 0.826x_{16} + 0.162x_{17} + 0.171x_{18} \\
 F_3 &= -0.028x_1 + 0.354x_2 - 0.187x_3 + 0.580x_4 + 0.249x_5 + 0.035x_6 + 0.087x_7 \\
 &\quad + 0.890x_8 - 0.255x_9 - 0.248x_{10} + 0.870x_{11} + 0.151x_{12} - 0.153x_{13} \\
 &\quad - 0.202x_{14} + 0.104x_{15} + 0.111x_{16} + 0.038x_{18} \\
 F_4 &= -0.025x_1 + 0.069x_2 - 0.047x_3 - 0.014x_4 - 0.073x_5 - 0.076x_6 - 0.076x_7 \\
 &\quad + 0.112x_8 + 0.233x_9 + 0.445x_{10} + 0.102x_{11} - 0.150x_{12} + 0.076x_{13} \\
 &\quad + 0.471x_{14} + 0.458x_{15} + 0.456x_{16} + 0.744x_{17} + 0.394x_{18} \\
 F_5 &= 0.031x_1 - 0.018x_2 + 0.025x_3 - 0.209x_4 - 0.279x_5 - 0.119x_6 - 0.144x_7 \\
 &\quad + 0.280x_8 + 0.746x_9 + 0.605x_{10} + 0.298x_{11} + 0.117x_{12} - 0.165x_{13} \\
 &\quad - 0.209x_{14} - 0.123x_{15} - 0.120x_{16} - 0.301x_{17} - 0.206x_{18} \\
 F_6 &= -0.005x_1 + 0.012x_2 - 0.009x_3 + 0.039x_4 + 0.011x_5 + 0.006x_6 + 0.009x_7 \\
 &\quad + 0.045x_8 + 0.055x_9 - 0.037x_{10} + 0.044x_{11} + 0.501x_{12} + 0.701x_{13} \\
 &\quad + 0.514x_{14} + 0.215x_{15} + 0.197x_{16} - 0.358x_{17} - 0.373x_{18} \\
 F &= \frac{\left(\begin{aligned} &31.474\% F_1 + 15.262\% F_2 + 13.086\% F_3 + 9.309\% F_4 \\ &+ 8.302\% F_5 + 7.602\% F_6 \end{aligned} \right)}{85.035\%}
 \end{aligned} \tag{13}$$

The running state trend diagram of the combined new parameter variable F in the whole life cycle of the rolling bearings is shown in Figure 7.

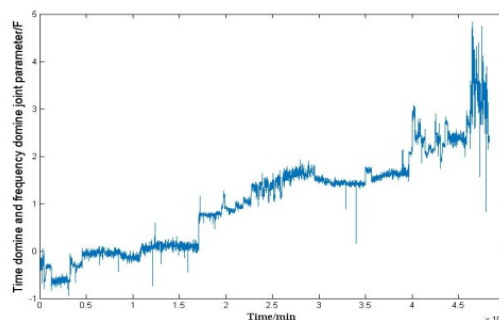


Figure 7. Trend of joint time domain and frequency domain parameters F .

Compared with Figure 5 and Figure 6, Figure 7 can combine the advantages of the two. According to the magnitude of the F amplitude, the entire trend graph can be divided into five stages. The amplitude of the first stage is less than 0. In the second stage, the amplitude of the first stable

period is around 0~0.3. It can be seen from the Figure 7 that the amplitude of the third stage is rising between 0.3~1.7. The fourth stage reaches the second stable amplitude of around 1.7~2.0. In the fifth stage, the amplitude is greater than 2.0, and the change drastically increased. It is consistent with the five life stages of the running-in period, normal operation, early failure, intermediate failure, and scrap phase of the rolling bearings, which proves that the feature parameter extraction is reasonable.

6. Experimental verification

Rolling bearings generally go through five stages of running-in period, stable period, pre-wear period, mid-wear period and scrap period during the whole life cycle. To verify the accuracy of the rolling bearing division in five different periods, several other groups of rolling bearings data in different periods are selected for inspection. The bearing type is N205EM, The experimental speed is 1500 rpm.

Figure 8 shows the new rolling bearing. Partial data during the running-in period of the rolling bearings without any external interference is shown in Table 7.

Table 7. Rolling bearing running-in period operation data sheet.

Parameter	Bearing					
	Bearing 1	Bearing 2	Bearing 3	Bearing 4	Bearing 5	Bearing 6
Maximum value	0.331266	0.173247	0.113838	0.115207	0.183048	0.172044
Minimum value	-0.284857	-0.220233	-0.106962	-0.104506	-0.15264	-0.16943
Variance	0.00253	0.001097	0.000323	0.000407	0.000944	0.001078
Skewness	0.049057	-0.105746	-0.047372	-0.063308	0.013716	-0.00918
Crest factor	6.585553	5.231315	6.331354	5.709636	5.956743	5.238983
Kurtosis value	3.668997	3.732743	3.647081	3.518312	3.493974	3.588518
Time domain synthesis parameters	-0.49000	-0.56000	-0.22000	-0.27000	-0.16000	-0.22000
Frequency domain average	2.420398	1.494328	1.551097	1.43708	2.382932	2.340677
Center of gravity frequency	13107680	13107694	13107626	13107008	13107569	13107698
Mean square frequency	242601	247075	249377	247021	247395	251026
Frequency domain amplitude variance	19.77534	4.901701	8.630995	5.966292	24.76375	23.63791
Frequency domain amplitude deviation index	1.85948	3.4177	9.33689	1.76058	4.18591	3.81385
Frequency domain amplitude kurtosis index	3.20801	1.65049	9.90682	3.4897	2.76785	2.01683
Frequency domain synthesis parameters	-0.21000	-0.75000	-0.52000	-1.17000	-0.05000	0.1000
Time domain and frequency domain joint parameter F	-0.33000	-0.62000	-0.77000	-0.58000	-0.26000	-0.11000



Figure 8. Normal operation of rolling bearing.

It can be known from Table 7 that the parameters of rolling bearings changed greatly and showed irregular changes during this period. This is because the rolling bearings are brand new and need to be run-in when the rolling bearing is running. By comparing with Figure 7, the data in this period is more consistent with the curve data in the interval of 0–6370 min, and the F values are less than 0, so the interval 0–6370 min is defined as the running-in period of the rolling bearing.

Some data parameters of rolling bearings after running for a period of time are shown in Table 8, which shows that the running state of the bearings during this period is relatively stable, and the value of each parameter changes little. Compared with Figure 7, it is consistent with the data in the period of 6380–14400 min. The F values are between 0–0.3, so the time period of 6380–14400 min is defined as the normal operating state of the rolling bearings.

Table 8. Rolling bearing normal operation data sheet.

Parameter	Bearing					
	Bearing 1	Bearing 2	Bearing 3	Bearing 4	Bearing 5	Bearing 6
Maximum value	0.202636	0.162332	0.165347	0.173321	0.128705	0.164781
Minimum value	-0.212514	-0.16602	-0.163767	-0.156167	-0.166876	-0.154671
Variance	0.001161	0.000971	0.000847	0.001087	0.000723	0.00075
Skewness	0.055004	0.028093	-0.005417	-0.013408	-0.321766	-0.096294
Crest factor	5.947209	5.210561	5.6803294	5.255964	4.786676	6.017099
Kurtosis value	3.256261	3.155725	3.140202	3.210032	3.4795607	3.449157
Time domain synthesis parameters	-0.11000	-0.19000	-0.170000	-0.22000	-0.400000	-0.190000
Frequency domain average	2.387279	2.000238	2.163854	1.361317	1.36316	1.707661
Center of gravity frequency	13107628	13107621	13107658	13106047	13107476	13107442
Mean square frequency	248774	255028	254376	267288	260661	259947
Frequency domain amplitude variance	24.41027	18.96061	21.95848	20.43021	17.31165	16.62991
Frequency domain amplitude deviation index	5.57064	4.54627	4.48288	1.22736	1.48396	7.77227
Frequency domain amplitude kurtosis index	4.00467	2.17408	2.07188	1.21409	1.81681	5.57238
Frequency domain synthesis parameters	0.01000	-0.04000	0.08000	-0.97000	-0.12000	-0.15000
Time domain and frequency domain joint parameter F	0.04000	0.07000	0.02000	0.09000	0.11000	0.08000

After the wear period and the stable operation period, in order to accelerate the change of the bearing life state, the artificially manufactured weak fault is shown in Figure 9. The size of the fault is 1.5 mm wide and 0.3 mm deep, which achieved early fault effects for experimental inspection. The experimental data are shown in Table 9.

Through the analysis of experimental data table 9 and Figure 7, we find that the running data of the rolling bearings change greatly during this period, and the amplitude is increasing. This is because the bearings are in a weak fault period, some parameters are more sensitive to the weak change of the fault. The experimental running data is in good agreement with the graph in the period from 14410 to 25680 minutes, and the F values are between 0.3 and 1.7, which can be regarded as a weak failure period of the rolling bearings.



Figure 9. Early fault bearing.

Table 9. Rolling bearing early fault operation data sheet.

Parameter	Bearing					
	Bearing 1	Bearing 2	Bearing 3	Bearing 4	Bearing 5	Bearing 6
Maximum value	0.136928	0.171925	0.10094	0.126128	0.285772	0.195407
Minimum value	-0.166927	-0.158232	-0.105178	-0.19991	-0.276312	-0.29886
Variance	0.000698	0.000707	0.000314	0.000492	0.000725	0.000657
Skewness	-0.064688	-0.083701	0.0864115	-0.331124	-0.360702	-0.480002
Crest factor	5.184182	6.467023	5.699646	5.685521	10.59265	7.622499
Kurtosis value	4.6170366	4.705728	3.797344	5.040614	9.541568	10.32127
Time domain synthesis parameters	-0.24000	-0.16000	-0.17000	-0.38000	0.16000	-0.21000
Frequency domain average	1.780924	1.712819	1.948742	1.94679	2.023343	1.514255
Center of gravity frequency	13107426	13107527	13107425	13107306	13107348	13107356
Mean square frequency	257100	238327	246384	249538	247544	159459
Frequency domain amplitude variance	18.86637	5.100236	9.826832	11.89232	11.62938	9.73649
Frequency domain amplitude deviation index	1.02093	1.70887	4.09601	3.5925	3.02614	4.17108
Frequency domain amplitude kurtosis index	9.85949	3.3904	2.21923	1.46234	8.53256	1.68545
Frequency domain synthesis parameters	-0.16000	5.39000	4.21000	3.46000	10.53000	3.68000
Time domain and frequency domain joint parameter F	0.39000	0.58000	0.85000	1.05000	0.12000	1.26000

The weak fault of the rolling bearings is further enlarged as shown in Figure 10. At this point, the fault size of the rolling bearings is 1.5 mm wide and 0.5 mm deep, which achieves the mid-term failure effect for experimental inspection. The experimental data is shown in Table 10.



Figure 10. Medium-term fault bearing.

Table 10. Rolling bearing medium-term fault operation data.

Parameter	Bearing					
	Bearing 1	Bearing 2	Bearing 3	Bearing 4	Bearing 5	Bearing 6
Maximum value	0.266835	0.266961	0.295686	0.252149	0.220223	0.233308
Minimum value	-0.30422	-0.281781	-0.353835	-0.256819	0.232719	-0.229089
Variance	0.001884	0.001538	0.002079	0.00122	0.00225	0.00125
Skewness	-0.000916	0.0003904	0.001545	-0.109245	-0.14790	-0.030627
Crest factor	6.1473811	6.807178	6.484634	7.217894	6.292714	6.599002
Kurtosis value	4.5581382	4.084713	5.0260825	4.1980203	4.074858	3.7748344
Time domain synthesis parameters	-0.05000	-0.04000	0.01000	-0.10000	-0.20000	-0.11000
Frequency domain average	3.793162	3.551865	3.865041	3.185822	3.353207	3.210801
Center of gravity frequency	13107535	13107557	13107519	13107456	13107463	13107377
Mean square frequency	240223	238722	243022	242403	236729	236386
Frequency domain amplitude variance	33.18258	24.94688	35.34664	19.82426	20.9332	20.028836
Frequency domain amplitude deviation index	2.81308	1.87654	2.14689	1.65154	1.49124	1.40468
Frequency domain amplitude kurtosis index	1.06817	4.48216	5.7188	3.35747	2.36756	1.810964
Frequency domain synthesis parameters	3.06000	6.48000	7.71000	5.35000	4.36000	3.81000
Time domain and frequency domain joint parameter F	1.85000	1.87000	1.89000	1.82000	1.92000	1.84000

After the bearings have experienced a weak failure, the wear degree of bearings has reached a relatively stable level. Therefore, the fluctuation of the parameters amplitude during this period is small, and the F value is fixed around 1.7–2. It is not difficult to analyze Table 10 and Figure 7 to find that the data in this period is consistent with 25690–35230min, which is called the middle stage of failure.

After the middle stage of the failure, the bearing operating state will enter the scrap period. In order to test the validity of the new parameters during this period, the fault location of the experimental bearing is further deepened, which reaches 4 mm wide and 1 mm deep. The bearing failure is shown in Figure 11, and the data of the experimental operation is shown in Table 11.

Table 11. Rolling bearing end-of-life operating data.

Parameter	Bearing					
	Bearing 1	Bearing 2	Bearing 3	Bearing 4	Bearing 5	Bearing 6
Maximum value	0.282937	0.243594	0.251703	0.44677	0.254331	0.15692
Minimum value	-0.268219	-0.254591	-0.283827	-0.410939	-0.191041	-0.153541
Variance	0.001693	0.001728	0.001806	0.002707	0.001436	0.000826
Skewness	-0.008151	-0.019024	-0.010563	0.381017	0.220984	-0.01772
Crest factor	6.876692	5.8600701	5.922669	8.586306	6.711062	5.4597156
Kurtosis value	3.656453	3.5916421	3.7451012	3.9067776	4.0683312	3.3649503
Time domain synthesis parameters	-0.05000	0.14000	-0.11000	0.54000	0.09000	-0.23000
Frequency domain average	3.72384	3.987033	2.00286	2.646099	2.754702	2.463502
Center of gravity frequency	13107391	13107499	13107348	13107527	13107482	13107654
Mean square frequency	240706	235222	265975	242920	241495	241769
Frequency domain amplitude variance	27.61894	28.94823	27.41521	16.54646	15.86649	20.45943
Frequency domain amplitude deviation index	1.95003	1.21156	1.02968	4.3311	3.96914	1.73312
Frequency domain amplitude kurtosis index	4.76684	1.52744	1.1359	2.17821	2.36453	2.3955
Frequency domain synthesis parameters	6.67000	3.51000	3.13000	4.17821	4.36453	4.3955
Time domain and frequency domain joint parameter F	2.17000	2.73000	3.05000	3.61000	4.02000	4.33000



Figure 11. Fault bearing in the end of life.

At this stage, rolling bearings failure is obvious. The parameter value is relatively large and the size is unstable. It is found through observation that when the time is 35240–48700 min in Figure 7, the data is similar to Table 11 and the F values are greater than 2, which is defined as the bearing scrap period.

Based on the abovementioned, the quantitative standard of F values can be shown in Table 12.

Table 12. New parameter F determines the quantitative standard of rolling bearing life state.

Period	0~6370min	6380~14400min	14410~25680min	25690~35230min	35240~48700min
Operating status	Run-in period	Stable period	Early fault	Medium-term fault	Scrap period fault
F value	<0	0~0.3	0.3~1.7	1.7~2	>2
Data characteristics	First down then up	Stable	Gradually rising	Stable	Rise sharply

7. Conclusion

The principal component analysis (PCA) is proposed to extract a new indicator in this paper which is the joint parameters of time domain and frequency domain. By using the new indicator of rolling bearings during operation, the operating conditions of rolling bearings can be clearly classified to five life stages: the running-in period, normal operation, early failure, intermediate failure, and scrap phase of the rolling bearings. And the classification results are basically consistent with the running status of the bearings. Therefore, it is feasible to use the PCA to carry out on-line monitoring and running status research of bearings.

Acknowledgments

This work was supported in part by the Natural Science Foundation of Liaoning Province under Grant 2019ZD0112 and 2019ZD0099, and in part by the National Natural Science Foundation of China under grant 51475065, grant 51605068, Traction Power State Key Laboratory of Southwest Jiaotong University under grant TPL2002, and Liaoning BaiQianWan Talents Program.

Conflicts of interest

The authors declare no conflict of interest.

References

1. H. Zhao, H. Liu, J. Xu, et al. *Performance prediction using high-order differential mathematical morphology gradient spectrum entropy and extreme learning machine*, IEEE T. Instrum. Meas., **69** (2020), 4165–4172.
2. S. Lu, P. Zheng, Y. Liu, et al. *Sound-aided vibration weak signal enhancement for bearing fault detection by using adaptive stochastic resonance*, J. Sound Vib., **449** (2019), 18–29.
3. T. Li, J. Shi, X. Li, et al. *Image encryption based on pixel-level diffusion with dynamic filtering and DNA-level permutation with 3D Latin cubes*, Entropy, **21** (2019), 1–21.
4. Y. Xu, H. Chen, J. Luo, et al. *Enhanced Moth-flame optimizer with mutation strategy for global optimization*, Inform. Sciences, **492** (2019), 181–203.

5. H. Zhao, J. Zheng, J. Xu, et al. *Fault diagnosis method based on principal component analysis and broad learning system*, IEEE Access, **7** (2019), 99263–99272.
6. H. Pan, Y. Yang, J. Zheng, et al. *A noise reduction method of symplectic singular mode decomposition based on Lagrange multiplier*, Mech. Syst. Signal Pr., **133** (2019), 1–21.
7. Q. Shu, S. Lu, M. Xia, et al. *Enhanced feature extraction method for motor fault diagnosis using low-quality vibration data from wireless sensor networks*, Meas. Sci. Technol., **31** (2020), 045016
8. R. Chen, S. K. Guo, X. Z. Wang, et al. *Fusion of multi-RSMOTE with fuzzy integral to classify bug reports with an imbalanced distribution*, IEEE T. Fuzzy Syst., **27** (2019), 2406–2420.
9. H. Zhao, S. Zuo, M. Hou, et al. *A novel adaptive signal processing method based on enhanced empirical wavelet transform technology*, Sensors, **18** (2018), 1–17.
10. Y. Liu, X. Wang, Z. Zhai, et al. *Timely daily activity recognition from headmost sensor events*, ISA T., **94** (2019), 379–390.
11. H. Zhao, J. Zheng, W. Deng, et al. *Semi-supervised broad learning system based on manifold regularization and broad network*, IEEE T. Circuits-I., **67** (2020), 983–994.
12. T. Li, Z. Qian, T. He, *Short-term load forecasting with improved CEEMDAN and GWO-based multiple kernel ELM*, Complexity, **2020** (2020), 1–20.
13. J. Zheng, Z. Dong, H. Pan, et al. *Composite multi-scale weighted permutation entropy and extreme learning machine based intelligent fault diagnosis for rolling bearing*, Measurement, **143** (2019), 69–80.
14. G. Xu, D. M. Hou, H. Qi, et al. *High-speed train wheel set bearing fault diagnosis and prognostics: A new prognostic model based on extendable useful life*, Mech. Syst. Signal Pr., **146** (2020), 1–23.
15. F. Zhang, J. Yan, P. Fu, et al. *Ensemble sparse supervised model for bearing fault diagnosis in smart manufacturing*, Mech. Syst. Signal Pr., **65** (2020), 1–11.
16. R. Liu, B. Yang, E. Zio, et al. *Artificial intelligence for fault diagnosis of rotating machinery: A review*, Mech. Syst. Signal Pr., **108** (2018), 33–47.
17. R. A. Carmona, W. L. Hwang, B. Torresani, *Characterization of signals by the ridges of their wavelet transforms*, IEEE T. Signal Proces., **45** (1997), 2586–2590.
18. W. Deng, H. Liu, J. Xu, et al. *An improved quantum-inspired differential evolution algorithm for deep belief network*, IEEE T. Instrum. Meas., **2020** (2020), 1–8.
19. H. Li, Y. Zhang, H. Zheng, *Hilbert-Huang transform and marginal spectrum for detection and diagnosis of localized defects in roller bearing*, J. Mech. Sci. Technol., **23** (2009), 291–301.
20. Y. Lei, J. Lin, Z. He, et al. *A review on empirical mode decomposition in fault diagnosis of rotating machinery*, Mech. Syst. Signal Pr., **35** (2013), 108–126.
21. Y. Wang, F. Liu, Z. Jiang, et al. *Complex variational mode decomposition for signal processing applications*, Mech. Syst. Signal Pr., **86** (2017), 75–85.
22. N. Lu, Z. Xiao, O. P. Malik, *Feature extraction using adaptive multiwavelets and synthetic detection index for rotor fault diagnosis of rotating machinery*, Mech. Syst. Signal Pr., **52** (2015), 393–415.
23. J. Zheng, H. Pan, S. Yang, et al. *Adaptive parameterless empirical wavelet transform based time-frequency analysis method and its application to rotor rubbing fault diagnosis*, Signal Process., **130** (2017), 305–314.
24. F. Cheng, J. Wang, L. Qu, et al. *Rotor-current-based fault diagnosis for DFIG wind turbine drivetrain gearboxes using frequency analysis and a deep classifier*, IEEE T. Ind. Appl., **54** (2017), 1062–1071.

25. H. Ocak, K. A. Loparo, *HMM-based fault detection and diagnosis scheme for rolling element bearings*, *J. Vib. Acoust.*, **127** (2005), 299–306.
26. N. Gebraeel, M. Lawley, R. Liu, et al. *Residual life predictions from vibration-based degradation signals: A neural network approach*, *IEEE T. Ind. Electron.*, **51** (2004), 694–700.
27. C. Sun, Z. Zhang, Z. He, *Research on bearing life prediction based on support vector machine and its application*, *J. Phys. Conf. Ser.*, **305** (2011), 1–9.
28. P. J. Vlok, M. Wnek, M. Zygmunt, *Utilising statistical residual life estimates of bearings to quantify the influence of preventive maintenance actions*, *Mech. Syst. Signal Pr.*, **18** (2004), 833–847.
29. X. Zhang, R. Xu, C. Kwan, et al. *An integrated approach to bearing fault diagnostics and prognostics*, In: *Proceedings of the 2005, American Control Conference*, 2005, 2750–2755.
30. S. Lu, Q. He, J. Wang, *A review of stochastic resonance in rotating machine fault detection*, *Mech. Syst. Signal Pr.*, **116** (2019), 230–260.
31. H. Zhao, D. Li, W. Deng, et al. *Research on vibration suppression method of alternating current motor based on fractional order control strategy*, *P. I. Mech. Eng. E-J. Pro.*, **231** (2017), 786–799.
32. Y. Shao, K. Nezu, *Prognosis of remaining bearing life using neural networks*, *P. I. Mech. Eng-I. Sys.*, **214** (2000), 217–230.
33. W. Deng, J. Xu, Y. Song, et al. *An effective improved co-evolution ant colony optimization algorithm with multi-strategies and its application*, *Int. J. Bio-Inspired Comput.*, **2019** (2019), 1–10.
34. H. Shao, J. Cheng, H. Jiang, et al. *Enhanced deep gated recurrent unit and complex wavelet packet energy moment entropy for early fault prognosis of bearing*, *Knowl-Based Syst.*, **188** (2020), 1–14.
35. H. Chen, Q. Zhang, J. Luo, et al. *An enhanced Bacterial Foraging Optimization and its application for training kernel extreme learning machine*, *Appl. Soft Comput.*, **86** (2020), 1–24.
36. W. Yang, M. Qian, D. Huang, *Detection of exons with deletions and insertions by hidden markov models*, *Prog. Biochem. Biophys.*, **29** (2002), 56–59.
37. W. Deng, J. Xu, H. Zhao, *An improved ant colony optimization algorithm based on hybrid strategies for scheduling problem*, *IEEE Access*, **7** (2019), 20281–20292.
38. Y. Liu, Y. Mu, K. Chen, et al. *Daily activity feature selection in smart homes based on pearson correlation coefficient*, *Neural Process. Lett.*, **51** (2020), 1771–1787.
39. Z. He, H. Shao, X. Zhang, et al. *Improved deep transfer auto-encoder for fault diagnosis of gearbox under variable working conditions with small training samples*, *IEEE Access*, **7** (2019), 115368–115377.
40. W. Deng, W. Li, X. Yang, *A novel hybrid optimization algorithm of computational intelligence techniques for highway passenger volume prediction*, *Expert Syst. Appl.*, **38** (2011), 4198–4205.
41. J. B. Ali, B. Chebel-Morello, L. Saidi, et al. *Accurate bearing remaining useful life prediction based on Weibull distribution and artificial neural network*, *Mech. Syst. Signal Pr.*, **56** (2015), 150–172.
42. M. Chen, Q. Li, *Application of oil pressure curve monitoring in sliding bearing wear diagnosis*, *Machine Tool & Hydraulics*, **21** (2010), 145–148.
43. B. Samanta, K. R. Al-Balushi, *Artificial neural network based fault diagnostics of rolling element bearings using time-domain features*, *Mech. Syst. Signal Pr.*, **17** (2003), 317–328.
44. Y. Zhang, S. Qin, *Fault detection of nonlinear processes using multiway kernel independent component analysis*, *Ind. Eng. Chem. Res.*, **46** (2007), 7780–7787.

45. A. Hyvärinen, E. Oja, *Independent component analysis: Algorithms and applications*, Neural Networks, **13** (2000), 411–430.
46. R. B. W. Heng, M. J. M. Nor, *Statistical analysis of sound and vibration signals for monitoring rolling element bearing condition*, Appl. Acoust., **53** (1998), 211–226.
47. N. Tandon, *A comparison of some vibration parameters for the condition monitoring of rolling element bearings*, Measurement, **12** (1994), 285–289.
48. R. Li, J. Chen, X. Wu, et al. *Fault diagnosis of rotating machinery based on SVD, FCM and RST*, Int. J. Adv. Manuf. Tech., **27** (2005), 128–135.
49. N. Gebraeel, M. Lawley, R. Liu, et al. *Vibration-based condition monitoring of thrust bearings for maintenance management*, In: *Proc. ANNIE 2002 Smart Engineering System Design: Neural Networks, Fuzzy Logic, Evolutionary Programming, Artificial Life and Data Mining*, 2002, 543–551.



AIMS Press

© 2020 the Author(s), licensee AIMS Press. This is an open access article distributed under the terms of the Creative Commons Attribution License (<http://creativecommons.org/licenses/by/4.0>)